actuators

MDPI

Review

Carbon Nanostructures for Actuators: An Overview of Recent Developments

Mauro Giorcelli and Mattia Bartoli *

Department of Applied Science and Technology (DISAT), Politecnico di Torino, Corso Duca degli Abruzzi 24, 10129 Torino, Italy; mauro.giorcelli@polito.it

* Correspondence: mattia.bartoli@polito.it; Tel.: +39-011-090-4326

Received: 3 April 2019; Accepted: 28 May 2019; Published: 2 June 2019

Abstract: In recent decades, micro and nanoscale technologies have become cutting-edge frontiers in material science and device developments. This worldwide trend has induced further improvements in actuator production with enhanced performance. A main role has been played by nanostructured carbon-based materials, i.e., carbon nanotubes and graphene, due to their intrinsic properties and easy functionalization. Moreover, the nanoscale decoration of these materials has led to the design of doped and decorated carbon-based devices effectively used as actuators incorporating metals and metal-based structures. This review provides an overview and discussion of the overall process for producing AC actuators using nanostructured, doped, and decorated carbon materials. It highlights the differences and common aspects that make carbon materials one of the most promising resources in the field of actuators.

Keywords: carbon nanotubes; fullerene; graphene; graphene oxide; actuators

1. Introduction

In the past twenty years, the research of new high-performance materials has gained a great deal of attention for sensor and actuator applications [1], mainly due to the development of industrial automation processes [2]. Also, the field of electronic engineering has required better performance for a large number of applications [3,4]. Since their discovery, allotropic carbon forms [5,6] emerged as the best candidates for the production of input–output devices [7] and electric transducers [8]. The great interest in carbon nanotubes (CNTs), fullerenes, and graphene is due to their astonishing mechanical, electrical, and electronic properties [9]. The use of nanostructured carbon-based materials has proven fruitful for developing a wide range of micro and nanodevices [10–12], with a particular focus on those able to produce tunable outputs [13]. Moreover, the high conductivity of aromatic conjugate systems of nanostructured carbon makes them excellent for the production of electrodes and electrochemistry applications [14–16]. Despite these superior properties, the high cost and difficult dispersion in other media have reduced their use for large-scale applications. A reasonable and technically affordable solution is the incorporation of nanostructured carbon-based materials into a wide polymeric matrix, trying to join the bulk properties of the polymers with the superior theoretical properties of nanostructured carbon-based materials [17]. Also, controlled chemical functionalization improves the processability as in the case of CNTs [18] and fullerenes [19], or when converting graphene into graphene oxide [20]. This review discusses the main recent achievements in the use of nanostructured carbon-based materials with a particular focus on the materials and their applications, and is organized as follows: (i) CNTs, (ii) graphene and graphene oxides, and (iii) fullerenes.

2. Molecular Actuation

Molecular actuation is the basis of all biological system locomotion ranging from bacteria [21] to human bodies [22]. Locomotion of living organisms is essentially based on the actuation promoted by protein activated through phosphorylation reactions [23]. Such big molecular conglomerates are elegant but hardly reproducible through common synthetic approaches. Several systems have been developed joining molecular actuation with affordable synthetic pathways. Among all of them, rotaxanes [24] and catenanes [25] are the most studied. Light stimuli actuation based on rotaxanes and catenanes is recognized worldwide as one of the most spectacular achievements in recent years, as demonstrated by the Nobel prize awarded in 2016 for molecular machine development. Other efficient and easy producible actuators are based on the isomerization of carbon–carbon double bonds in highly hindered aromatic molecules [26].

Despite their astonishing properties, all synthetic molecular actuators are lacking in scalability due to the need for multistep synthesis and working conditions. Polymers and polymer composite-based actuators comprise the majority of molecular actuators combining versatility and effectiveness [27–29]. The following sections provide a brief overview on nanostructured carbon-based polymeric actuators.

3. Nanostructured Carbon: Effective Tools for Carbon-Based Nanoactuators

3.1. Carbon Nanotube-Based Actuators

CNTs are carbon allotropic forms with a high aspect ratio [30] classified into two main families (i) single-walled CNTs (SWCNTs) and (ii) multiwalled CNTs (MWCNTs), according to the number of concentric cylindrical structures of which they are composed, as shown in Figure 1.

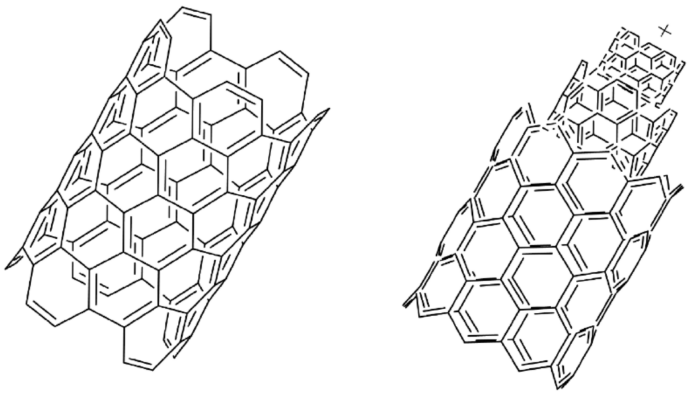

(**a**) (**b**)

Figure 1. Longitudinal section of (**a**) single-walled carbon nanotube (SWCNT) and (**b**) multiwalled carbon nanotube (MWCNT).

Since the development of the first nanoelectromechanical systems, CNTs have attracted great interest as they combine theoretical superior mechanical and electronic properties [31–33]. One of the most important properties of CNTs is that they are very good conductors of both electricity and heat. Their high aspect ratio also provides a valid advantage when compared to other carbon nanostructures such as cage compounds [34]. CNTs are also very strong and elastic molecules in certain directions, and all of these properties are difficult to find combined at the same time in one material. For current carbon nanotube actuators, multiwalled carbon nanotubes (MWCNTs) and bundles of MWCNTs have been widely used, mostly due to ease of handling and robustness if compared with SWCNTs, i.e., highly oriented CNTs on single molecule devices such as nanoscale rotation actuators [35–37].

3.2. Graphene and Graphene Oxide

Graphene is an extremely electrically conductive form of elemental carbon that is composed of a single flat sheet of carbon atoms arranged in a repeating hexagonal lattice. The term graphene is also used to identify carbon sheets formed by double or multilayers because high quality and defect free single layer graphene is extremely difficult to create and manipulate. Today, graphene and graphene oxide, as shown in Figure 2, are considered next-generation materials [38]. Since the pioneering work of Stankovich et al. [39], graphene-based composites present excellent properties such as high electrical [40] and thermal conductivity. The particular characteristics of graphene are conductivity, transparency, and mechanical resistance, a very large specific surface area (theoretical value of 2630 m^2/g) [41], and its electron-rich double-sided polycyclic aromatic scaffold, making it a promising material for different applications, included actuators [42,43].

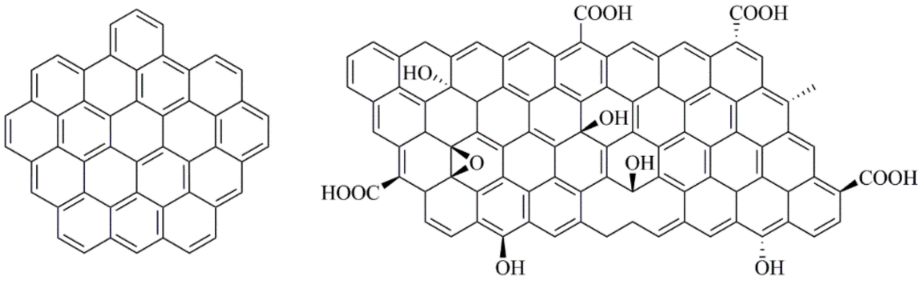

(**a**) (**b**)

Figure 2. Scheme of a single layer of (**a**) graphene or (**b**) graphene oxide.

3.3. Fullerene-Based Actuators

Among all the exotic allotropic carbon forms, fullerene-shaped forms are the smallest in size and the highest in strain [44], allowing efficient cycloaddition reactions on their surface [45]. Fullerene was clearly identified using mass spectroscopy in 1985 by Kroto et al. [46] who aimed to explain adsorption observed in the interstellar medium. After its discovery, the first rational synthesis of C_{60} was reported by Krätschmer et al. [47] in 1990.

Among different fullerenes illustrated in Figure 3, C_{60} has gained much attention due to its chemical reactivity [48], hydrogen storage capability [49], and for the six one-by-one-electron reduction behavior [50]. These attractive properties are counterbalanced by a very high cost that inhibits C_{60} use at a large scale. Nonetheless, fullerenes have been investigated for different applications as actuators because of their properties, such as high surface area, thermal stability, non-toxicity, biocompatibility, and hydrophilic functionalization. Despite these, fullerenes are characterized by a high resistivity, close to 1014 Ω/m [51], compared with CNT or high quality graphene that could reach a value of down to 10^{-6} Ω/m [52,53].

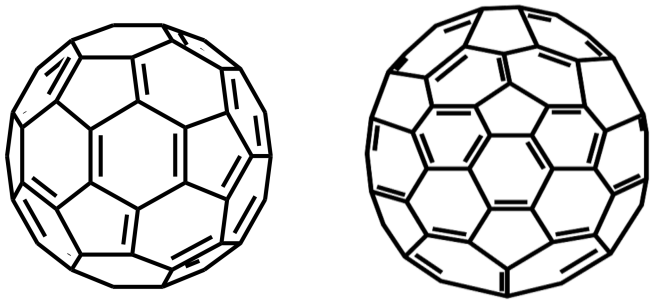

(**a**) (**b**)

Figure 3. (**a**) Shape of fullerene C_{60}, also known as buckyball, and (**b**) fullerene C_{70}. As clearly evident, not all fullerenes are characterized by the same symmetry.

4. Applications

4.1. Carbon Nanotube-Based Actuators

CNTs are used to produce actuators that exploit their different properties when pristine or in composites. The first actuation using CNTs was reported by Baughman et al. [54], where a sheet of aggregated SWCNTs named buckypaper achieved a displacement of 0.12% under a square wave potential of ±0.5 V. A few years later, Roth et al. [55] reported electrochemical actuation on a single CNT and a maximum isometric stress of up to 25 MPa [56]. Many studies have been devoted to investigating the relationship between electrical input and the actuations of CNTs [57,58], showing how the aspect ratio is an unneglectable factor together with the network properties of CNTs [49,59,60].

Further observations were reported by Senga et al. [61] using a transmission electron microscope to prove the transition between the flattened state and the tubular state in rather thick CNTs, enlightening the relationship with thermal energy.

Other examples of actuators based on nanotube structures use the electroactuation process that induces deformation on CNTs using electrical stimuli [62–65]. Some example of CNT-based actuators are shown in Figure 4.

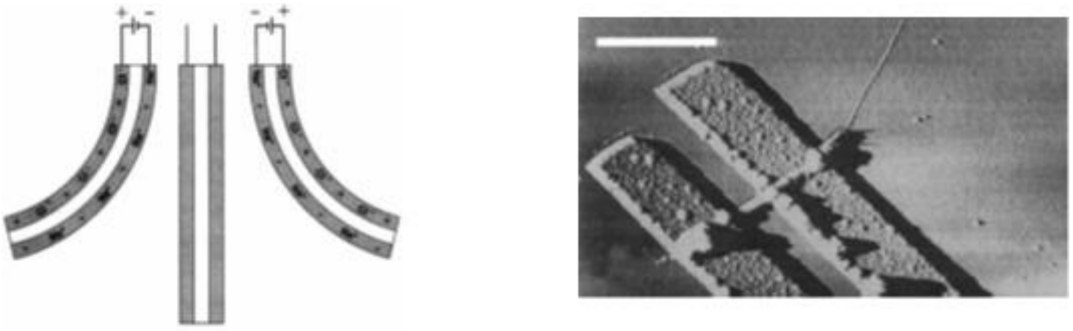

Figure 4. Examples of actuators based on pristine carbon nanotubes (CNTs), (**left**) from by Baughman et al. [54], (**right**) from Roth et al. [55].

The combined use of ionic liquids together with CNTs and polymers is a well-established practice able to obtain well-dispersed gels [66,67], as reported by Sugino et al. [68]. They also described the benefits of the simultaneous use of SWCNTS/ionic liquids and a conductive polymeric additive, and reported a triplicate strain value [69] using a mix of ionic surfactants compared with a non-additive actuator. Terasawa et al. [70] used a non-ionic surfactant to produce a CNT-containing gel. In this case, actuation was performed using poly(vinylidene fluoride-co-hexafluoropropylene) or poly(ethylene oxide) materials, with the latter showing better performance. A model based on ionic transport number and the ionic volume was proposed to explain this behavior, proving that the self-diffusion coefficient, rate of ion transport in the electrodes, and electrolyte types are all critical factors for this type of actuation.

Nevertheless, among all CNT polymer composites, elastomers are among the most studied [71]. Fang et al. [72] used dielectric elastomers mixed with highly aligned SWCNTs sheets modified using a laser treatment to induce mechanical anisotropy. During the electrochemical actuation, this treatment showed an appreciable beneficial effect reaching a strain of up to 33%. Anisotropic actuation was also used to develop soft linear actuators [73] operating at a low electrical field (100 V/μm) comprising a SWCNT electrode supported onto an acrylic matrix, inducing a strain of up to 40% in dielectric electroactive polymers. Among these last polymers, sulfonated fluoropolymers (e.g., Nafion) have generated great interest due to their simple synthesis and filming properties [74]. Lian et al. [75] induced actuation using functionalized SWCNTs dispersed into a Nafion matrix with a concentration doubling the storage modulus and the strain compared with the neat matrix. Similarly, Lu et al. [76] used carboxylic derivatives of SWCNTs supported onto carbon fibers for the production

of Nafion–silica-based shape memory polymers. In this case, both electrical and thermally induced actuation was performed and magnified by the presence of SWCNTs. Layering was a common technique in SWCNT-based actuation. Mukai et al. [77] reported the use of a millimetric layer of SWCNTs as support for the growth of poly(pyrrole) by electropolymerization, performing the actuation in a watery medium with a displacement of around 0.1%. A three-layered structure was studied by Sachyani et al. [78], which promoted an angular strain of 300° attributed to unaligned SWCNTs together with a flexible polymer layer. As reported by Zhang et al. [79], non-conductive polymers could be used as components for actuators. In this recent study, a transparency actuator based on a single layer super-aligned SWCNT sheet and paraffin–poly(dimethylsiloxane) matrix was developed showing a displacement of up to 0.4% with a switchable transmittance. High-performing polymers, such as polyimides, could also be used to produce tough actuator devices. As suggested by Ning et al. [80], pre-dispersed SWCNTs could be used to produce highly aligned CNT matrices supported onto a polyimide film and used as a thermomechanical actuator. A multiresponsive actuator was described by Zhou et al. [81]. In this case, super-aligned SWCNTs were used to produce a U-shaped device able to show twisting deformation under both thermal and electrical stimuli. Moreover, SWCNTs could be combined with other carbon sources, such as carbides [82], or inorganic species [83] improving the responses of the actuators by up to 60% [84].

MWCNTs have been used more widely for actuation than SWCNTs. Capeluto et al. [85] described the use of MWCNTs combined with azopolymers to produce transparent film actuators. Recently, Ji et al. [86] used MWCNTs/poly(dimethylsiloxane) to produce a very thick film able to generate a linear strain actuation of up to 4% under high voltage (100 V). Poly(pyrrole) was also used with a high load of MWCNTs (of up to 25 wt %) with a displacement after actuation of up to 18% [87]. Shirasu et al. [88] reported an actuation by using a thermoset polymer. In their study, a U-shaped epoxy-based device was produced, dispersing aligned MWCNTs and inducing a bending displacement of up to 10% under an applied DC voltage of 6 V. Further, MWCNTs were obtained with ruthenium oxides and the resulting inorganic-containing carbon material was used as an actuator, doubling the performances of a unfunctionalized SWCNTs based device considering the strain and maximum generated stress [89]. Better performances of MWCNTs containing actuators were reported for 1-ethyl-3-methylimidazolium tetrafluoroborate ionic liquid-based systems [90] compared with carbon black-based devices, showing a strain improvement of up to 0.8%.

The use of a randomly distributed CNT net is an affordable approach to combine actuation capability avoiding the alignment procedure reported above. Chen et al. reported two interesting examples using buckypaper/Nafion actuators [91], or without a polymer matrix under very high voltage (1100V) [92]. In both cases, a good actuation response was observed of up to 1%.

4.2. Graphene and Graphene Oxide Actuators

Graphene actuation was studied by Saane and Onck [93] using a Density Functional Theory (DFT) calculation based on an adaptive intermolecular reactive empirical bond order potential method. The authors demonstrated the better performances of graphene compared to the inorganic material used (nanoporous gold), achieving a smaller actuation stroke under an electrical field but generating an enhanced mechanical work. Graphene-based composites used as electroactive actuators are reported to be highly sensitive to electric stimuli showing a monotonic response to electrical solicitations [94]. As seen in Figure 5, graphene–Nafion membrane actuators represent a good benchmark for comparing properties, such as mechanical strength between devices, with a displacement of up to 60% [95]. As a result of this, graphene was also used to developed wearable poly(pyrrole)-based fibers employed for the production of net actuators [96]. Sen et al. [97] reported the actuation of cellulose using graphene nanoplatelets (0.1–0.5 wt %) under DC excitation voltages of 3–7 V, reaching a strain of up to 1%. Titanium-doped graphene was used to induce actuation into an elastomeric matrix with a strain of up to 72% using 39 V/μm [98]. Graphene-based actuators are able to induce actuation under

different external stimuli. Liu et al. [99] performed a photochemical actuation on bilayered graphene nanoplatelets/poly(dimethylsiloxane) using a near infrared light, as shown in Figure 5.

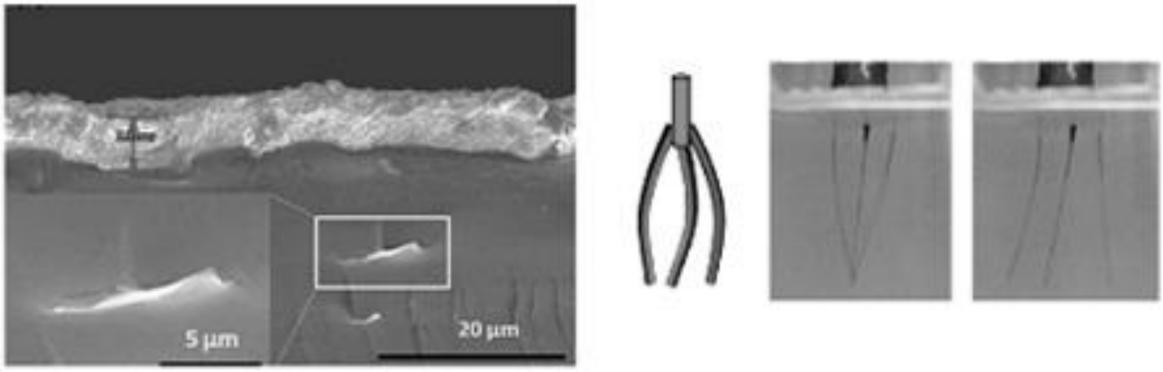

Figure 5. (**Left**) Graphene–Nafion membrane (thickness ~0.34 mm) from [95] and (**right**) snapshots of the tri-armed tweezers made by graphene fiber/polypyrrole (GF/PPy) driven by an applied electrical potential from [96].

The main unsolved issue in the use of graphene is the poor dispersion in polymeric matrices. An affordable solution could be heteroatomic massive functionalization [100] as in the case of graphene oxide (GO). Oxidized graphite has been well known about since the first studies reported by Brodie in the middle of the 19th century [101], but oxidative protocols have only allowed the production of GO in recent years [102]. GO showed a better dispersibility with respect to common graphene, producing very stable solutions in watery and polar solvents media [103].

Actuators based on GO were easily produced using hydrogels receiving both thermal and UV stimuli [104]. Actuation using near infrared light was performed by Chen et al. [105] using GO and poly(*N*-isopropylacrylamide) with remarkably shape memory. Similar results were obtained using Nafion-based materials [106]. Effective interactions between residual groups of GO and polar functionalities was proved using actuators composed by sulfonated poly(styrene) [107] or poly(pyrrole) [108], reaching a bending angle greater than 360 °C using low voltage (around 1 V). Recently, Vural et al. [109] produced a tandem bimorph actuator based on proteins and GO, reaching a maximum curvature three times higher than conventional GO of up to 17%. Terasawa et al. [110], combined GO and vapor-grown carbon fibers in an ionic liquid medium obtaining an actuation improvement of 56% compared with the same system containing SWCNTs. The high capacity for oxygen-based functionalities of GO enabled production of a very interesting bioinspired high-performance dielectric elastomer actuator, based on titanate supported onto poly(dopamine) GO. This material mimics a mussel shell, showing a very high actuation response to electrical stimulation with a strain of up to 1%, applying a 2 V triangular voltage frequency. Wang et al. [111] described a multiresponsive PDMS/graphene composite able to perform the actuation under different chemical stimuli with an exceptional recovery property of up to 98% after three cycles.

Another interesting property of GO is related to the possibility of high-ordered material production through direct reduction of GO. Reduced GO (rGO) has properties quite close to pristine graphene together with a considerable price reduction and its versatility permits the production of various actuator devices. As an example, Selvakumar et al. [112] described a biomorphic electrical actuator based on an rGO analog of CNTs buckypaper. A similar study was reported by Wang et al. [113] using an epoxy matrix producing a shape memory material with very high recoverability after hundreds of cycles. Other research reported visible light actuation induced by rGO on chitosan polymer, producing high-performance actuation [114] of up to 4% displacement.

4.3. Fullerene-Based Actuators

As mentioned before, the interesting properties of fullerene (high surface area, porosity, thermal stability, non-toxicity, bio-compatibility, and hydrophilic functionalization) are used to produce actuators. Kaur et al. [115] reported the use of low fullerene species (C_{20}) studying actuation at a molecular level using a purely theoretical approach based on DFT non-equilibrium charge transport (DFT-NEGF) computation method.

A similar study was reported by Huang et al. [116] using scandium nitride encapsulated into C_{80}, proposing its use for single-molecule memory and logic devices for parallel molecular computing architectures.

A proper device was described by Jung et al. [117] assembling a C_{60}–Nafion membrane that showed a harmonic response to an oscillating electrical field as shown in Figure 6. A more complex system was produced by Panwar et al. [118] using oxygenated C_{60}. The fullerene-based electrode was anchored to an elastomeric matrix composed of poly(vinylidene fluoride)/poly(vinylpyrrolidone)/sulfonated poly(styrene) enhancing the actuation response.

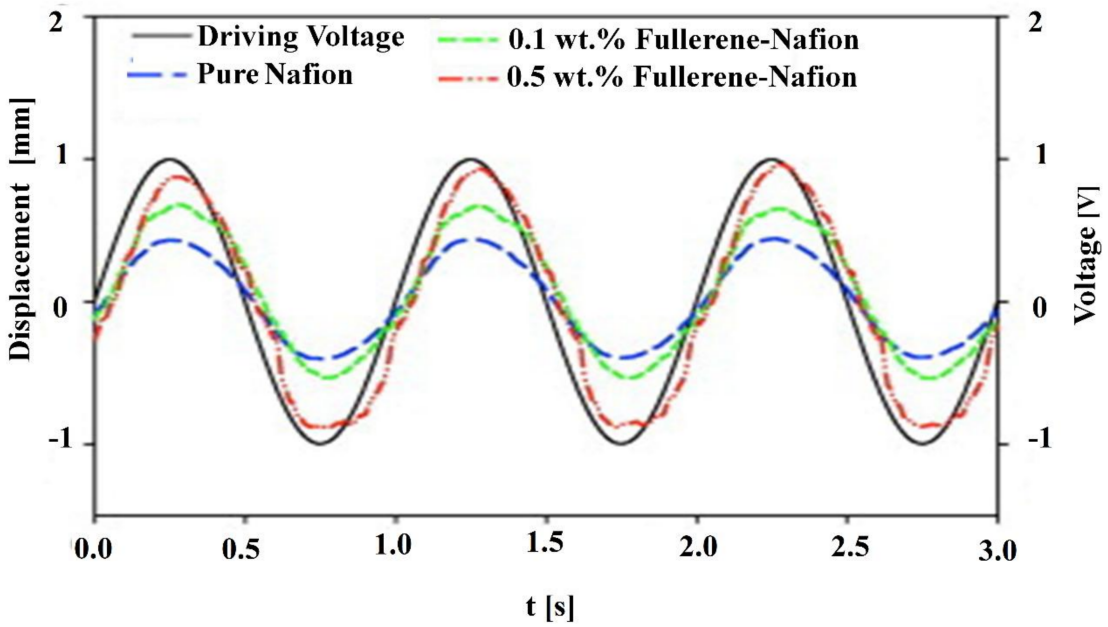

Figure 6. Displacement of fullerene-based actuators in function of 1 V driving voltage [117].

5. Challenges and Prospective of Actuators Based on Carbon Nanostructures

Actuators based on carbon materials represent a field that is evolving day by day. Challenges are found in the field of biology, such as in nanomanipulation, where actuators with high performance are requested. An important aspect to take in account is the economical aspect. CNTs, graphene, and fullerene are expensive materials with low reproducibility. These drawbacks become a problem for large-scale application, where the economical aspect is not secondary to the material reproducibility in the case of standardization processes. Researchers are studying new carbon materials with low costs and high reproducibility grades able to demonstrate comparable performances to expensive carbon materials such as biochar, that are actually used only for sensor production [119]. Moreover, the ecofriendly aspect—which is not currently being addressed for the production of CNTs, graphene, and fullerene—will play an increasing role in the future production of actuators [120].

6. Conclusions

Nanoscale and macroscopic carbon-based actuation is a vast and very promising field with potentially great impact on device applications [121–124]. Combined with the lack of suitable molecular

actuators, the use of CNTs and graphene/rGO materials could exploit novel actuation technologies. The further development of allotropic-containing materials poses viable exciting challenges which lie ahead.

Nevertheless, the main issue to be taken into account in the use of CNTs, graphene, and fullerene in any containing material is the economical drawback. These considerations discourage the use of nanostructured carbon material, but the astonishing performances showed by all of the allotropic carbon forms leave the door open for future evolution.

In conclusion, nanostructured carbon-based actuators have been studied extensively under small-scale and lab conditions and shown promising performances, but have not yet achieved their full potential.

Acknowledgments: Mauro Giorcelli wants to thank the MODCOMP project (grant 685844, European H2020 program) for financial support.

Conflicts of Interest: The authors declare no conflict of interest.

References

1. Vanderborght, B.; Albu-Schäffer, A.; Bicchi, A.; Burdet, E.; Caldwell, D.G.; Carloni, R.; Catalano, M.; Eiberger, O.; Friedl, W.; Ganesh, G. Variable impedance actuators: A review. *Robot. Auton. Syst.* **2013**, *61*, 1601–1614. [CrossRef]
2. Jammes, F.; Smit, H. Service-oriented paradigms in industrial automation. *IEEE Trans. Ind. Inform.* **2005**, *1*, 62–70. [CrossRef]
3. Kirkam, H. Optical current transducers for power systems: A review. *IEEE Trans. Power Deliv.* **1994**, *9*, 1778–1788.
4. Kovacs, G.T. *Micromachined Transducers Sourcebook*; McGraw-Hill Science Engineering: New York, NY, USA, 1998.
5. Terrones, M.; Hsu, W.K.; Kroto, H.W.; Walton, D.R. Nanotubes: A Revolution in Materials Science and Electronics. In *Fullerenes and Related Structures*; Springer: New York, NY, USA, 1999; pp. 189–234.
6. Kroto, H. C_{60} Buckminsterfullerene, other fullerenes and the icospiral shell. *Comput. Math. Appl.* **1989**, *17*, 417–423. [CrossRef]
7. Cataldo, F. The impact of a fullerene-like concept in carbon black science. *Carbon* **2002**, *40*, 157–162. [CrossRef]
8. Wang, J. Carbon-nanotube based electrochemical biosensors: A review. *Electroanal. Int. J. Devoted Fundam. Pract. Asp. Electroanal.* **2005**, *17*, 7–14. [CrossRef]
9. Malik, S. Structural and electronic properties of nano-carbon materials such as graphene, nanotubes and fullerenes. *Nature* **1985**, *318*, 162–163.
10. Heerema, S.J.; Dekker, C. Graphene nanodevices for DNA sequencing. *Nat. Nanotechnol.* **2016**, *11*, 127–136. [CrossRef]
11. Kamat, P.V.; Guldi, D.M.; D'Souza, F. *Fullerenes and Nanotubes: The Building Blocks of Next Generation Nanodevices: Proceedings of the International Symposium on Fullerenes, Nanotubes, and Carbon Nanoclusters*; The Electrochemical Society: Pennington, NJ, USA, 2003.
12. Matsuo, Y.; Nakamura, E. Application of fullerenes to nanodevices. *Chem. Nanocarbons* **2010**, 173–187. [CrossRef]
13. Choi, J.; Pyo, S.; Baek, D.-H.; Lee, J.-I.; Kim, J. Thickness-, alignment- and defect-tunable growth of carbon nanotube arrays using designed mechanical loads. *Carbon* **2014**, *66*, 126–133. [CrossRef]
14. Ghasemi, M.; Daud, W.R.W.; Hassan, S.H.; Oh, S.-E.; Ismail, M.; Rahimnejad, M.; Jahim, J.M. Nano-structured carbon as electrode material in microbial fuel cells: A comprehensive review. *J. Alloys Compd.* **2013**, *580*, 245–255. [CrossRef]
15. Gooding, J.J. Nanostructuring electrodes with carbon nanotubes: A review on electrochemistry and applications for sensing. *Electrochim. Acta* **2005**, *50*, 3049–3060. [CrossRef]
16. Zhang, Y.; Feng, H.; Wu, X.; Wang, L.; Zhang, A.; Xia, T.; Dong, H.; Li, X.; Zhang, L. Progress of electrochemical capacitor electrode materials: A review. *Int. J. Hydrog. Energy* **2009**, *34*, 4889–4899. [CrossRef]
17. Li, C.; Thostenson, E.T.; Chou, T.-W. Sensors and actuators based on carbon nanotubes and their composites: A review. *Compos. Sci. Technol.* **2008**, *68*, 1227–1249. [CrossRef]

18. Ma, P.-C.; Siddiqui, N.A.; Marom, G.; Kim, J.-K. Dispersion and functionalization of carbon nanotubes for polymer-based nanocomposites: A review. *Compos. Part A Appl. Sci. Manuf.* **2010**, *41*, 1345–1367. [CrossRef]
19. Patil, A.; Schriver, G.; Carstensen, B.; Lundberg, R. Fullerene functionalized polymers. *Polym. Bull.* **1993**, *30*, 187–190. [CrossRef]
20. Zhu, Y.; Murali, S.; Cai, W.; Li, X.; Suk, J.W.; Potts, J.R.; Ruoff, R.S. Graphene and graphene oxide: Synthesis, properties, and applications. *Adv. Mater.* **2010**, *22*, 3906–3924. [CrossRef]
21. Berg, H.C. How bacteria swim. *Sci. Am.* **1975**, *233*, 36–45. [CrossRef]
22. Adelstein, R.S.; Conti, M.A.; Barylko, B. The role of myosin phosphorylation in regulating actin-myosin interaction in human blood platelets. *Thromb. Haemost.* **1978**, *39*, 241–244. [CrossRef]
23. Krebs, E.G.; Kent, A.B.; Fischer, E.H. The muscle phosphorylase b kinase reaction. *J. Biol. Chem.* **1958**, *231*, 73–83.
24. Wenz, G.; Han, B.-H.; Müller, A. Cyclodextrin rotaxanes and polyrotaxanes. *Chem. Rev.* **2006**, *106*, 782–817. [CrossRef]
25. Schill, G. *Catenanes, Rotaxanes, and Knots*; Elsevier: Amsterdam, The Netherlands, 2017; Volume 22.
26. Zhang, Y.; Ma, Y.; Sun, J. Reversible actuation of polyelectrolyte films: Expansion-induced mechanical force enables cis–trans isomerization of azobenzenes. *Langmuir* **2013**, *29*, 14919–14925. [CrossRef] [PubMed]
27. Madden, J.D.; Kanigan, T.S.; Lafontaine, S.; Hunter, I.W. Conducting Polymer Actuator. U.S. Patent Application No. 6,249,076B1, 19 June 2001.
28. Maitland, D.J.; Lee, A.P.; Schumann, D.L.; Matthews, D.L.; Decker, D.E.; Jungreis, C.A. Shape Memory Polymer Actuator and Catheter. U.S. Patent Application No. 6,740,094B2, 25 May 2004.
29. Noh, T.-G.; Tak, Y.; Nam, J.-D.; Choi, H. Electrochemical characterization of polymer actuator with large interfacial area. *Electrochim. Acta* **2002**, *47*, 2341–2346. [CrossRef]
30. Wang, X.; Li, Q.; Xie, J.; Jin, Z.; Wang, J.; Li, Y.; Jiang, K.; Fan, S. Fabrication of ultralong and electrically uniform single-walled carbon nanotubes on clean substrates. *Nano Lett.* **2009**, *9*, 3137–3141. [CrossRef] [PubMed]
31. Yu, M.; Dyer, M.J.; Skidmore, G.D.; Rohrs, H.W.; Lu, X.; Ausman, K.D.; Von Ehr, J.R.; Ruoff, R.S. Three-dimensional manipulation of carbon nanotubes under a scanning electron microscope. *Nanotechnology* **1999**, *10*, 244–252. [CrossRef]
32. Majumdar, S.; Lin, J.; Link, T.; Millard, J.; Augat, P.; Ouyang, X.; Newitt, D.; Gould, R.; Kothari, M.; Genant, H. Fractal analysis of radiographs: Assessment of trabecular bone structure and prediction of elastic modulus and strength. *Med. Phys.* **1999**, *26*, 1330–1340. [CrossRef]
33. Kasumov, A.Y.; Khodos, I.; Ajayan, P.; Colliex, C. Electrical resistance of a single carbon nanotube. *EPL (Europhys. Lett.)* **1996**, *34*, 429–434. [CrossRef]
34. Krueger, A. *Carbon Materials and Nanotechnology*; John Wiley & Sons: New York, NY, USA, 2010.
35. Hu, Y.; Chen, W.; Lu, L.; Liu, J.; Chang, C. Electromechanical actuation with controllable motion based on a single-walled carbon nanotube and natural biopolymer composite. *ACS Nano* **2010**, *4*, 3498–3502. [CrossRef]
36. Narendar, S. Mathematical modelling of rotating single-walled carbon nanotubes used in nanoscale rotational actuators. *Def. Sci. J.* **2011**, *61*, 317–324. [CrossRef]
37. Deng, J.; Li, J.; Chen, P.; Fang, X.; Sun, X.; Jiang, Y.; Weng, W.; Wang, B.; Peng, H. Tunable photothermal actuators based on a pre-programmed aligned nanostructure. *J. Am. Chem. Soc.* **2015**, *138*, 225–230. [CrossRef]
38. Geim, A.K.; Novoselov, K.S. The rise of graphene. In *Nanoscience and Technology: A Collection of Reviews from Nature Journals*; World Scientific: Singapore, 2010; pp. 11–19.
39. Stankovich, S.; Dikin, D.A.; Dommett, G.H.; Kohlhaas, K.M.; Zimney, E.J.; Stach, E.A.; Piner, R.D.; Nguyen, S.T.; Ruoff, R.S. Graphene-based composite materials. *Nature* **2006**, *442*, 282–286. [CrossRef] [PubMed]
40. Charlier, J.C.; Issi, J.P. Electrical conductivity of novel forms of carbon. *J. Phys. Chem. Solids* **1996**, *57*, 957–965. [CrossRef]
41. Stoller, M.D.; Park, S.; Zhu, Y.; An, J.; Ruoff, R.S. Graphene-based ultracapacitors. *Nano Lett.* **2008**, *8*, 3498–3502. [CrossRef] [PubMed]
42. Smith, A.T.; LaChance, A.M.; Zeng, S.; Liu, B.; Sun, L. Synthesis, properties, and applications of graphene oxide/reduced graphene oxide and their nanocomposites. *Nano Mater. Sci.* **2019**, *1*, 31–47. [CrossRef]
43. Xu, Z. Chapter 4—Fundamental properties of graphene. In *Graphene*; Zhu, H., Xu, Z., Xie, D., Fang, Y., Eds.; Academic Press: New York, NY, USA, 2018; pp. 73–102.

44. Dresselhaus, M.S.; Dresselhaus, G.; Eklund, P.C. *Science of Fullerenes and Carbon Nanotubes: Their Properties and Applications*; Elsevier: Amsterdam, The Netherlands, 1996.
45. Guldi, D.; Martin, N. Functionalized fullerenes: Synthesis and functions. *Compr. Nanosci. Nanotechnol.* **2019**, *187–191*.
46. Kroto, H.W.; Heath, J.R.; O'Brien, S.C.; Curl, R.F.; Smalley, R.E. C_{60}: Buckminsterfullerene. *Nature* **1985**, *318*, 162–163. [CrossRef]
47. Krätschmer, W.; Lamb, L.D.; Fostiropoulos, K.; Huffman, D.R. Solid C_{60}: A new form of carbon. *Nature* **1990**, *347*, 354–358. [CrossRef]
48. Biagiotti, G.; Cicchi, S.; De Sarlo, F.; Machetti, F. Reactivity of [60] fullerene with primary nitro compounds: Addition or catalysed condensation to isoxazolo [60] fullerenes. *Eur. J. Org. Chem.* **2014**, *2014*, 7906–7915. [CrossRef]
49. Chen, J.; Wu, F. Review of hydrogen storage in inorganic fullerene-like nanotubes. *Appl. Phys. A* **2004**, *78*, 989–994. [CrossRef]
50. Echegoyen, L.; Echegoyen, L.E. Electrochemistry of fullerenes and their derivatives. *Acc. Chem. Res.* **1998**, *31*, 593–601. [CrossRef]
51. Yadav, B.C.; Kumar, R. Structure, properties and applications of fullerenes. *Int. J. Nanotechnol. Appl.* **2008**, *2*, 15–24.
52. Lekawa-Raus, A.; Patmore, J.; Kurzepa, L.; Bulmer, J.; Koziol, K. Electrical properties of carbon nanotube based fibers and their future use in electrical wiring. *Adv. Funct. Mater.* **2014**, *24*, 3661–3682. [CrossRef]
53. Sun, H.-B.; Ge, G.; Zhu, J.; Hailong, Y.; Lu, Y.; Wu, Y.; Wan, J.; Han, M.; Luo, Y. High electrical conductivity of graphene-based transparent conductive films with silver nanocomposites. *RSC Adv.* **2015**, *5*, 108044–108049. [CrossRef]
54. Baughman, R.H.; Cui, C.; Zakhidov, A.A.; Iqbal, Z.; Barisci, J.N.; Spinks, G.M.; Wallace, G.G.; Mazzoldi, A.; De Rossi, D.; Rinzler, A.G. Carbon nanotube actuators. *Science* **1999**, *284*, 1340–1344. [CrossRef] [PubMed]
55. Roth, S.; Baughman, R.H. Actuators of individual carbon nanotubes. *Curr. Appl. Phys.* **2002**, *2*, 311–314. [CrossRef]
56. Baughman, R.H.; Zakhidov, A.A.; De Heer, W.A. Carbon nanotubes—The route toward applications. *Science* **2002**, *297*, 787–792. [CrossRef]
57. Fakhrabadi, M.M.S.; Rastgoo, A.; Ahmadian, M.T. Size-dependent instability of carbon nanotubes under electrostatic actuation using nonlocal elasticity. *Int. J. Mech. Sci.* **2014**, *80*, 144–152. [CrossRef]
58. Fakhrabadi, M.M.S.; Rastgoo, A.; Ahmadian, M.T. Non-linear behaviors of carbon nanotubes under electrostatic actuation based on strain gradient theory. *Int. J. Non Linear Mech.* **2014**, *67*, 236–244. [CrossRef]
59. Suppiger, D.; Busato, S.; Ermanni, P. Characterization of single-walled carbon nanotube mats and their performance as electromechanical actuators. *Carbon* **2008**, *46*, 1085–1090. [CrossRef]
60. Geier, S.M.; Mahrholz, T.; Wierach, P.; Sinapius, M. Morphology- and ion size-induced actuation of carbon nanotube architectures. *Int. J. Smart Mater.* **2018**, *9*, 111–134. [CrossRef]
61. Senga, R.; Hirahara, K.; Yamaguchi, Y.; Nakayama, Y. Carbon nanotube torsional actuator based on transition between flattened and tubular states. *J. Non-Cryst. Solids* **2012**, *358*, 2541–2544. [CrossRef]
62. Giménez, P.; Mukai, K.; Asaka, K.; Hata, K.; Oike, H.; Otero, T.F. Capacitive and faradic charge components in high-speed carbon nanotube actuator. *Electrochim. Acta* **2012**, *60*, 177–183. [CrossRef]
63. Hung, N.T.; Nugraha, A.R.T.; Saito, R. Three-dimensional carbon Archimedean lattices for high-performance electromechanical actuators. *Carbon* **2017**, *125*, 472–479. [CrossRef]
64. Hung, N.T.; Nugraha, A.R.T.; Saito, R. Charge-induced electrochemical actuation of armchair carbon nanotube bundles. *Carbon* **2017**, *118*, 278–284. [CrossRef]
65. Ouakad, H.M.; Sedighi, H.M. Rippling effect on the structural response of electrostatically actuated single-walled carbon nanotube based NEMS actuators. *Int. J. Non-Linear Mech.* **2016**, *87*, 97–108. [CrossRef]
66. Frolov, A.I.; Kirchner, K.; Kirchner, T.; Fedorov, M.V. Molecular-scale insights into the mechanisms of ionic liquids interactions with carbon nanotubes. *Faraday Discuss.* **2012**, *154*, 235–247. [CrossRef] [PubMed]
67. Fukushima, T.; Aida, T. Ionic liquids for soft functional materials with carbon nanotubes. *Chem. A Eur. J.* **2007**, *13*, 5048–5058. [CrossRef]
68. Sugino, T.; Shibata, Y.; Kiyohara, K.; Asaka, K. Actuation mechanism of dry-type polymer actuators composed by carbon nanotubes and ionic liquids. *Sens. Actuators B Chem.* **2018**, *273*, 955–965. [CrossRef]

69. Sugino, T.; Kiyohara, K.; Takeuchi, I.; Mukai, K.; Asaka, K. Actuator properties of the complexes composed by carbon nanotube and ionic liquid: The effects of additives. *Sens. Actuators B Chem.* **2009**, *141*, 179–186. [CrossRef]
70. Terasawa, N.; Hayashi, Y.; Koga, T.; Higashi, N.; Asaka, K. High-performance polymer actuators based on poly(ethylene oxide) and single-walled carbon nanotube–ionic liquid-based gels. *Sens. Actuators B Chem.* **2014**, *202*, 382–387. [CrossRef]
71. Pelrine, R.; Kornbluh, R.; Joseph, J.; Heydt, R.; Pei, Q.; Chiba, S. High-field deformation of elastomeric dielectrics for actuators. *Mater. Sci. Eng. C* **2000**, *11*, 89–100. [CrossRef]
72. Fang, X.; Li, A.; Yildiz, O.; Shao, H.; Bradford, P.D.; Ghosh, T.K. Enhanced anisotropic response of dielectric elastomer actuators with microcombed and etched carbon nanotube sheet electrodes. *Carbon* **2017**, *120*, 366–373. [CrossRef]
73. Cakmak, E.; Fang, X.; Yildiz, O.; Bradford, P.D.; Ghosh, T.K. Carbon nanotube sheet electrodes for anisotropic actuation of dielectric elastomers. *Carbon* **2015**, *89*, 113–120. [CrossRef]
74. Yeo, S.C.; Eisenberg, A. Physical properties and supermolecular structure of perfluorinated ion-containing (Nafion) polymers. *J. Appl. Polym. Sci.* **1977**, *21*, 875–898. [CrossRef]
75. Lian, H.; Qian, W.; Estevez, L.; Liu, H.; Liu, Y.; Jiang, T.; Wang, K.; Guo, W.; Giannelis, E.P. Enhanced actuation in functionalized carbon nanotube–Nafion composites. *Sens. Actuators B Chem.* **2011**, *156*, 187–193. [CrossRef]
76. Lu, H.; Yin, J.; Xu, B.; Gou, J.; Hui, D.; Fu, Y. Synergistic effects of carboxylic acid-functionalized carbon nanotube and Nafion/silica nanofiber on electrical actuation efficiency of shape memory polymer nanocomposite. *Compos. Part B Eng.* **2016**, *100*, 146–151. [CrossRef]
77. Mukai, K.; Yamato, K.; Asaka, K.; Hata, K.; Oike, H. Actuator of double layer film composed of carbon nanotubes and polypyrroles. *Sens. Actuators B Chem.* **2012**, *161*, 1010–1017. [CrossRef]
78. Sachyani, E.; Layani, M.; Tibi, G.; Avidan, T.; Degani, A.; Magdassi, S. Enhanced movement of CNT-based actuators by a three-layered structure with controlled resistivity. *Sens. Actuators B Chem.* **2017**, *252*, 1071–1077. [CrossRef]
79. Zhang, W.; Weng, M.; Zhou, P.; Chen, L.; Huang, Z.; Zhang, L.; Liu, C.; Fan, S. Transparency-switchable actuator based on aligned carbon nanotube and paraffin-polydimethylsiloxane composite. *Carbon* **2017**, *116*, 625–632. [CrossRef]
80. Ning, W.; Wang, Z.; Liu, P.; Zhou, D.; Yang, S.; Wang, J.; Li, Q.; Fan, S.; Jiang, K. Multifunctional super-aligned carbon nanotube/polyimide composite film heaters and actuators. *Carbon* **2018**, *139*, 1136–1143. [CrossRef]
81. Zhou, Z.-W.; Yan, Q.-H.; Liu, C.-H.; Fan, S.-S. An arm-like electrothermal actuator based on superaligned carbon nanotube/polymer composites. *New Carbon Mater.* **2017**, *32*, 411–418. [CrossRef]
82. Palmre, V.; Torop, J.; Arulepp, M.; Sugino, T.; Asaka, K.; Jänes, A.; Lust, E.; Aabloo, A. Impact of carbon nanotube additives on carbide-derived carbon-based electroactive polymer actuators. *Carbon* **2012**, *50*, 4351–4358. [CrossRef]
83. Gendron, D.; Bubak, G.; Ceseracciu, L.; Ricciardella, F.; Ansaldo, A.; Ricci, D. Significant strain and force improvements of single-walled carbon nanotube actuator: A metal chalcogenides approach. *Sens. Actuators B Chem.* **2016**, *230*, 673–683. [CrossRef]
84. Torop, J.; Arulepp, M.; Leis, J.; Punning, A.; Johanson, U.; Palmre, V.; Aabloo, A. Nanoporous carbide-derived carbon material-based linear actuators. *Materials* **2010**, *3*, 9–25. [CrossRef]
85. Capeluto, M.G.; Salvador, R.F.; Eceiza, A.; Goyanes, S.; Ledesma, S.A. Azopolymer film as an actuator for organizing multiwall carbon nanotubes. *Opt. Mater.* **2017**, *66*, 247–252. [CrossRef]
86. Ji, X.; El Haitami, A.; Sorba, F.; Rosset, S.; Nguyen, G.T.M.; Plesse, C.; Vidal, F.; Shea, H.R.; Cantin, S. Stretchable composite monolayer electrodes for low voltage dielectric elastomer actuators. *Sens. Actuators B Chem.* **2018**, *261*, 135–143. [CrossRef]
87. Rasouli, H.; Naji, L.; Hosseini, M.G. The effect of MWCNT content on electropolymerization of PPy film and electromechanical behavior of PPy electrode-based soft actuators. *J. Electroanal. Chem.* **2017**, *806*, 136–149. [CrossRef]
88. Shirasu, K.; Yamamoto, G.; Inoue, Y.; Ogasawara, T.; Shimamura, Y.; Hashida, T. Development of large-movements and high-force electrothermal bimorph actuators based on aligned carbon nanotube reinforced epoxy composites. *Sens. Actuators A Phys.* **2017**, *267*, 455–463. [CrossRef]

89. Galantini, F.; Bianchi, S.; Castelvetro, V.; Gallone, G. Functionalized carbon nanotubes as a filler for dielectric elastomer composites with improved actuation performance. *Smart Mater. Struct.* **2013**, *22*, 055025. [CrossRef]
90. Terasawa, N.; Ono, N.; Mukai, K.; Koga, T.; Higashi, N.; Asaka, K. High performance polymer actuators based on multi-walled carbon nanotubes that surpass the performance of those containing single-walled carbon nanotubes: Effects of ionic liquid and composition. *Sens. Actuators B Chem.* **2012**, *163*, 20–28. [CrossRef]
91. Chen, I.W.P.; Cottinet, P.-J.; Tsai, S.-Y.; Foster, B.; Liang, R.; Wang, B.; Zhang, C. Improved performance of carbon nanotube buckypaper and ionic-liquid-in-Nafion actuators for rapid response and high durability in the open air. *Sens. Actuators B Chem.* **2012**, *171–172*, 515–521. [CrossRef]
92. Chen, I.W.P.; Liang, Z.; Wang, B.; Zhang, C. Charge-induced asymmetrical displacement of an aligned carbon nanotube buckypaper actuator. *Carbon* **2010**, *48*, 1064–1069. [CrossRef]
93. Saane, S.S.R.; Onck, P.R. Atomistic modeling of the stiffness, strength and charge-induced actuation of graphene nanofoams. *Extrem. Mech. Lett.* **2015**, *5*, 54–61. [CrossRef]
94. Tungkavet, T.; Seetapan, N.; Pattavarakorn, D.; Sirivat, A. Graphene/gelatin hydrogel composites with high storage modulus sensitivity for using as electroactive actuator: Effects of surface area and electric field strength. *Polymer* **2015**, *70*, 242–251. [CrossRef]
95. Jung, J.-H.; Jeon, J.-H.; Sridhar, V.; Oh, I.-K. Electro-active grapheme—Nafion actuators. *Carbon* **2011**, *49*, 1279–1289. [CrossRef]
96. Wang, Y.; Bian, K.; Hu, C.; Zhang, Z.; Chen, N.; Zhang, H.; Qu, L. Flexible and wearable graphene/polypyrrole fibers towards multifunctional actuator applications. *Electrochem. Commun.* **2013**, *35*, 49–52. [CrossRef]
97. Sen, I.; Seki, Y.; Sarikanat, M.; Cetin, L.; Gurses, B.O.; Ozdemir, O.; Yilmaz, O.C.; Sever, K.; Akar, E.; Mermer, O. Electroactive behavior of graphene nanoplatelets loaded cellulose composite actuators. *Compos. Part B Eng.* **2015**, *69*, 369–377. [CrossRef]
98. Chen, T.; Qiu, J.; Zhu, K.; Li, J. Electro-mechanical performance of polyurethane dielectric elastomer flexible micro-actuator composite modified with titanium dioxide-graphene hybrid fillers. *Mater. Des.* **2016**, *90*, 1069–1076. [CrossRef]
99. Liu, H.; Niu, D.; Jiang, W.; Zhao, T.; Lei, B.; Yin, L.; Shi, Y.; Chen, B.; Lu, B. Illumination-oriented and thickness-dependent photomechanical bilayer actuators realized by graphene-nanoplatelets. *Sens. Actuators A Phys.* **2016**, *239*, 45–53. [CrossRef]
100. Jiang, D.; Zhu, H.; Yang, W.; Cui, L.; Liu, J. One-side non-covalent modification of CVD graphene sheet using pyrene-terminated PNIPAAm generated via RAFT polymerization for the fabrication of thermo-responsive actuators. *Sens. Actuators B Chem.* **2017**, *239*, 193–202. [CrossRef]
101. Brodie, B.C., XIII. On the atomic weight of graphite. *Philos. Trans. R. Soc. Lond.* **1859**, *149*, 249–259.
102. Hummers, W.S.J.; Offeman, R.E. Preparation of graphitic oxide. *J. Am. Chem. Soc.* **1958**, *80*, 1339. [CrossRef]
103. Dreyer, D.R.; Park, S.; Bielawski, C.W.; Ruoff, R.S. The chemistry of graphene oxide. *Chem. Soc. Rev.* **2010**, *39*, 228–240. [CrossRef] [PubMed]
104. Guo, L.; Hao, Y.-W.; Yang, P.; Li, P.-L.; Sun, N.; Feng, X.-W.; Zhao, J.; Chen, C.-A.; Song, J.-F. Fast fabrication of graphene oxide/reduced graphene oxide hybrid hydrogels for thermosensitive smart actuator utilizing laser irradiation. *Mater. Lett.* **2019**, *237*, 245–248. [CrossRef]
105. Chen, Z.; Cao, R.; Ye, S.; Ge, Y.; Tu, Y.; Yang, X. Graphene oxide/poly (N-isopropylacrylamide) hybrid film-based near-infrared light-driven bilayer actuators with shape memory effect. *Sens. Actuators B Chem.* **2018**, *255*, 2971–2978. [CrossRef]
106. Surana, K.; Singh, P.K.; Bhattacharya, B.; Verma, C.S.; Mehra, R.M. Synthesis of graphene oxide coated Nafion membrane for actuator application. *Ceram. Int.* **2015**, *41*, 5093–5099. [CrossRef]
107. Lee, J.-W.; Kwon, T.; Kang, Y.; Han, T.H.; Cho, C.G.; Hong, S.M.; Hwang, S.-W.; Koo, C.M. Styrenic block copolymer/sulfonated graphene oxide composite membranes for highly bendable ionic polymer actuators with large ion concentration gradient. *Compos. Sci. Technol.* **2018**, *163*, 63–70. [CrossRef]
108. Liu, A.; Yuan, W.; Shi, G. Electrochemical actuator based on polypyrrole/sulfonated graphene/graphene tri-layer film. *Thin Solid Films* **2012**, *520*, 6307–6312. [CrossRef]
109. Vural, M.; Lei, Y.; Pena-Francesch, A.; Jung, H.; Allen, B.; Terrones, M.; Demirel, M.C. Programmable molecular composites of tandem proteins with graphene oxide for efficient bimorph actuators. *Carbon* **2017**, *118*, 404–412. [CrossRef]
110. Terasawa, N.; Asaka, K. High-performance graphene oxide/vapor-grown carbon fiber composite polymer actuator. *Sens. Actuators B Chem.* **2018**, *255*, 2829–2837. [CrossRef]

111. Wang, W.; Zhang, Y.-L.; Han, B.; Ma, J.-N.; Wang, J.-N.; Han, D.-D.; Ma, Z.-C.; Sun, H.-B. A complementary strategy for producing moisture and alkane dual-responsive actuators based on graphene oxide and PDMS bimorph. *Sens. Actuators B Chem.* **2019**, *290*, 133–139. [CrossRef]
112. Selvakumar, D.; Alsalme, A.; Alghamdi, A.; Jayavel, R. Reduced graphene oxide paper as bimorphic electrical actuators. *Mater. Lett.* **2017**, *191*, 182–185. [CrossRef]
113. Wang, W.; Liu, D.; Liu, Y.; Leng, J.; Bhattacharyya, D. Electrical actuation properties of reduced graphene oxide paper/epoxy-based shape memory composites. *Compos. Sci. Technol.* **2015**, *106*, 20–24. [CrossRef]
114. Muralidharan, M.N.; Shinu, K.P.; Seema, A. Optically triggered actuation in chitosan/reduced graphene oxide nanocomposites. *Carbohydr. Polym.* **2016**, *144*, 115–121. [CrossRef]
115. Kaur, R.P.; Engles, D. Transport in a fullerene terminated aromatic molecular device. *J. Sci. Adv. Mater. Devices* **2018**, *3*, 206–212. [CrossRef]
116. Huang, T.; Zhao, J.; Feng, M.; Popov, A.A.; Yang, S.; Dunsch, L.; Petek, H. A multi-state single-molecule switch actuated by rotation of an encapsulated cluster within a fullerene cage. *Chem. Phys. Lett.* **2012**, *552*, 1–12. [CrossRef]
117. Jung, J.-H.; Vadahanambi, S.; Oh, I.-K. Electro-active nano-composite actuator based on fullerene-reinforced Nafion. *Compos. Sci. Technol.* **2010**, *70*, 584–592. [CrossRef]
118. Panwar, V.; Ko, S.Y.; Park, J.-O.; Park, S. Enhanced and fast actuation of fullerenol/PVDF/PVP/PSSA based ionic polymer metal composite actuators. *Sens. Actuators B Chem.* **2013**, *183*, 504–517. [CrossRef]
119. Jagdale, P.; Ziegler, D.; Rovere, M.; Tulliani, J.M.; Tagliaferro, A. Waste coffee ground biochar: A material for humidity sensors. *Sensors* **2019**, *19*, 801. [CrossRef]
120. Pourhashem, G.; Hung, S.Y.; Medlock, K.B.; Masiello, C.A. Policy support for biochar: Review and recommendations. *GCB Bioenergy* **2019**, *11*, 364–380. [CrossRef]
121. Wang, Y.; Fang, L.; Xiang, L.; Wu, G.; Zeng, Y.; Chen, Q.; Wei, X. On-chip thermionic electron emitter arrays based on horizontally aligned single-walled carbon nanotubes. *IEEE Trans. Electron Devices* **2019**, *66*, 1069–1074. [CrossRef]
122. Qiu, S.; Wu, K.; Gao, B.; Li, L.; Jin, H.; Li, Q. Solution-processing of high-purity semiconducting single-walled carbon nanotubes for electronics devices. *Adv. Mater.* **2019**, *31*, 1800750. [CrossRef] [PubMed]
123. Materón, E.M.; Lima, R.S.; Joshi, N.; Shimizu, F.M.; Oliveira, O.N.J. Graphene-containing microfluidic and chip-based sensor devices for biomolecules. In *Graphene-Based Electrochemical Sensors for Biomolecules*; Elsevier: Amsterdam, The Netherlands, 2019; pp. 321–336.
124. Tseng, L.-T.; Kazazis, D.; Wang, X.; Popescu, C.M.; Robinson, A.P.; Ekinci, Y. Sub-20 nm Si fins with high aspect ratio via pattern transfer using fullerene-based spin-on-carbon hard masks. *Microelectron. Eng.* **2019**, *210*, 8–13. [CrossRef]